THE ASTROPHYSICAL JOURNAL, 258:533–547, 1982 July 15

THE EXCITATION OF INTERSTELLAR C_2

EWINE F. VAN DISHOECK
Sterrewacht, Leiden

AND

JOHN H. BLACK
Harvard-Smithsonian Center for Astrophysics
Received 1981 September 21; accepted 1982 January 6

ABSTRACT

A theory is developed to describe the excitation of the diatomic carbon molecule in interstellar clouds. The probabilities of quadrupole transitions within the ground state and of intercombination transitions between levels of the lowest triplet and singlet states are computed. The populations of excited rotational levels can be used as a diagnostic probe of local temperature, density, and strength of the radiation field, although all three parameters cannot usually be determined from C_2 data alone. Calculated rotational populations are presented for a range of physical conditions and are used to interpret existing interstellar absorption line observations of C_2. Because of the competition between radiative and collisional excitation processes, the rotational excitation temperature tends not to be a good measure of kinetic temperature. An unusual radio frequency spectrum of C_2 is predicted.

Subject headings: interstellar: molecules — molecular processes — transition probabilities

I. INTRODUCTION

The observation of weak interstellar absorption lines in the wavelength region 8000–12000 Å has been made possible by the development of image intensifiers and photon-counting detectors which are sensitive in this region. Significant achievements in this area include the discovery of new diffuse interstellar bands (Sanner, Snell, and Vanden Bout 1978) and the first detection of interstellar diatomic carbon, C_2 (Souza and Lutz 1977). C_2 is a particularly important molecule because the relative populations of its long-lived ground-state rotational levels are measurable and can be sensitive diagnostic probes of conditions in the clouds that produce the interstellar absorption lines. The interpretation of the observations of rotationally excited H_2 has provided useful information about the densities, temperatures, and ultraviolet radiation fields in diffuse interstellar clouds (Spitzer and Jenkins 1975; Black and Dalgarno 1973, 1976; Glassgold and Langer 1974; Jura 1975*a*, *b*). The excitation processes in C_2 and H_2 are analogous, and it is expected that C_2 will be a similarly valuable diagnostic. Although the lines of the less abundant carbon molecule are weaker than those of H_2, the relation between measured equivalent widths and column densities is more straightforward. C_2 also has the advantage that some of its strong absorption lines lie in the far red and near-infrared parts of the spectrum and are accessible to telescopes on Earth, while the lines of H_2 in the far-ultraviolet must be observed from spacecraft. Moreover, the extinction per unit column density of interstellar matter is much smaller in the far red than in the far-ultraviolet, so that C_2 can potentially be observed in thicker interstellar clouds than can H_2.

The gas-phase processes responsible for the formation of interstellar C_2 were identified by Watson (1974*a*, *b*). Abundances of C_2 were predicted for the diffuse clouds toward ζ Oph (Black and Dalgarno 1977) and ζ Per (Black, Hartquist, and Dalgarno 1978) on the basis of detailed chemical models. These predictions agreed well with subsequent near-infrared and ultraviolet observations of C_2 toward these stars (Snow 1978; Chaffee and Lutz 1978; Hobbs 1979; Chaffee *et al.* 1980). C_2 has also been observed toward several other stars (Hobbs 1981; Souza 1979; Cosmovici and Strafella 1981).

A preliminary discussion of the theory of rotational excitation in interstellar C_2 was presented by Chaffee *et al.* (1980). In the present paper we survey in detail the molecular processes that govern the excitation of C_2 (§ II), and we present a theoretical description of rotational populations (§ III) for use in interpreting observations (§ IV).

II. MOLECULAR PROPERTIES AND PROCESSES

a) *The Ground-State Quadrupole Moment of* C_2

Because C_2 is a homonuclear species having no permanent dipole moment, radiative transitions between vibration-rotation levels of the same electronic state can

occur only as slow, electric quadrupole transitions. In order to calculate the probabilities of such transitions, it is necessary to know the quadrupole moment, $Q(R)$, as a function of internuclear separation, R. This function can be computed from accurate ab initio theoretical wavefunctions.

The ab initio calculations were performed using the ALCHEMY system of programs developed by P. S. Bagus, B. Liu, A. D. McLean, and M. Yoshimine. A rather large Slater-type basis set was employed in the present study; it consisted of the $(6s/4p)$ set of Clementi and Roetti (1974) augmented by two $3d$ functions (exponents 2.0 and 1.0) and one $4f$ function (exponent 2.0) on each C atom. The computed energy for the $X\ ^1\Sigma_g^+$ state at the equilibrium internuclear separation, $R_e = 2.348$ bohr, is -75.4056 hartree with this basis in a self-consistent field (SCF) calculation.[1] The quadrupole moment of a linear molecule is defined as

$$Q(R) = \sum_k Z_k R_k^2 - \left\langle \Psi_0(r;R) \left| \sum_i r_i^2 P_2(\cos\theta_i) \right| \Psi_0(r;R) \right\rangle \quad \text{atomic units.} \quad (1)$$

Here k sums over all nuclei, R_k is the distance of nucleus k from the coordinate origin (which lies on the molecular axis), and Z_k is the charge on nucleus k. Ψ_0 is the computed wave function of the $X\ ^1\Sigma_g^+$ state at internuclear distance R, r stands collectively for the positions of all electrons, $P_2(\cos\theta) = 3/2\cos^2\theta - 1/2$, and i sums over all electrons located at distances r_i from the coordinate origin at angles θ_i with respect to the molecular axis. The integration in the second term is over the electronic coordinates. For a homonuclear molecule, Q is independent of the origin of the coordinate system. The computed quadrupole moment of C_2 at SCF level is $Q(R_e) = 2.78$ au at R_e. The addition of the $4f$ functions to the basis set did not alter the quadrupole moment by more than 2% over the entire range of internuclear distances considered.

The SCF calculation was followed by a moderately large configuration-interaction (CI) calculation containing approximately 1850 configuration state functions (CSF) which were selected in the following way. First, the molecular orbitals which resulted from the SCF calculation for the $X\ ^1\Sigma_g^+$ state were divided into core $(1\sigma_g, 1\sigma_u)$, internal $(2\sigma_g, 2\sigma_u, 3\sigma_g, 3\sigma_u, 1\pi_g, 1\pi_u)$, and external $(4\sigma_g - 10\sigma_g, 4\sigma_u - 10\sigma_u, 2\pi_g - 5\pi_g, 2\pi_u - 5\pi_u, 1\delta_g, 1\delta_u)$ orbitals. The following CSF were then included in the final CI calculation:

1. All CSF arising from the distribution of the eight valence electrons in the internal space (the core orbitals were always kept doubly occupied); this is also called a Full Valence CI (FVCI).

2. All CSF arising from single excitations into the external space with respect to the following five reference configurations:

a) $(1\sigma_g)^2(1\sigma_u)^2(2\sigma_g)^2(2\sigma_u)^2(1\pi_u)^4$;
b) $(1\sigma_g)^2(1\sigma_u)^2(2\sigma_g)^2(3\sigma_g)^2(1\pi_u)^4$;
c) $(1\sigma_g)^2(1\sigma_u)^2(2\sigma_g)^2(2\sigma_u)^2(1\pi_u)^2(1\pi_g)^2$;
d) $(1\sigma_g)^2(1\sigma_u)^2(2\sigma_g)^2(2\sigma_u)^1(3\sigma_g)^1(1\pi_u)^3(1\pi_g)^1$;
e) $(1\sigma_g)^2(1\sigma_u)^2(2\sigma_g)^2(2\sigma_u)^2(1\pi_g)^4$.

3. All CSF arising from double excitations into the external space with respect to reference configuration (a).

Approximate natural orbitals were obtained by diagonalization of the calculated density matrix. The CI calculation was then repeated using these natural orbitals. The calculated CI energies at equilibrium internuclear distance are -75.5308 hartree for the FVCI calculation, -75.6532 hartree for the large CI calculation using $X\ ^1\Sigma_g^+$ molecular orbitals, and -75.6781 hartree for the large CI calculation using natural orbitals. The corresponding values for the quadrupole moment at R_e are 2.18 au, 2.34 au, and 2.26 au, respectively. From this it appears that the CI calculations using natural orbitals should give a quadrupole moment function accurate to 10% at $R \lesssim R_e$. At larger R, the uncertainties may be somewhat greater since the calculation did not include configurations arising from double excitations with respect to configurations (c) and (d). The quadrupole moment as a function of R for the $X\ ^1\Sigma_g^+$ state is presented in Table 1 and Figure 1. The error limit on the point at $R_e = 2.348$ bohrs indicates the estimated accuracy of $Q(R)$. The classical turning points of vibrational states $v = 0$–5 lie between $R = 2.06$ and $R = 2.78$ bohrs.

TABLE 1

GROUND-STATE QUADRUPOLE MOMENT OF C_2

R (bohr)	$Q(R)$ (atomic units)
1.75	0.82
2.00	1.43
2.20	1.91
2.348	2.26±0.1
2.60	2.82
2.80	3.23
3.00	3.60
3.50	4.08
4.00	4.20
4.50	3.91
6.00	3.25

[1]The atomic units of length, energy, and quadrupole moment are 1 bohr = 0.529177158 Å, 1 hartree = 219474.5529 cm^{-1} = 27.21 eV, and 1.34504×10^{-26} esu cm^2, respectively.

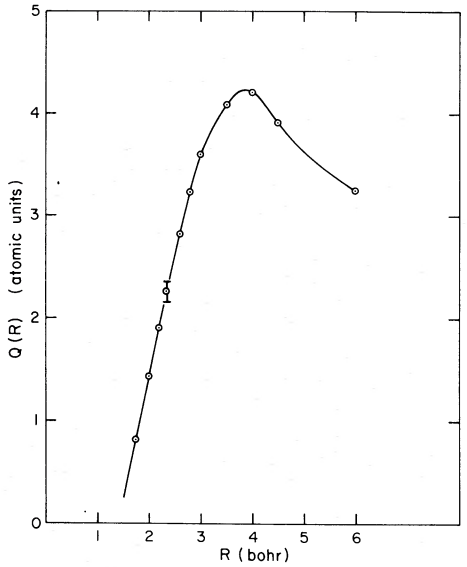

FIG. 1.—The adopted CI quadrupole moment of C_2 as a function of internuclear separation.

b) Quadrupole Transitions

The probability (Einstein A coefficient) of an electric quadrupole transition from upper state $v'J'$ to lower state $v''J''$ is

$$A(v'J', v''J'') = \frac{32\pi^6}{5h}\tilde{\nu}^5 S_Q(v'J', v''J'')/(2J'+1) \quad s^{-1}, \tag{2}$$

where J is the rotational quantum number, v is the vibrational quantum number, $\tilde{\nu}$ is the frequency of the transition in wavenumbers (cm^{-1}), and the line strength is defined as

$$S_Q(v'J', v''J'') = S_Q(v''J'', v'J') = \sum_{M'}\sum_{M''} |\langle v'J'M'|Q(R)|v''J''M''\rangle|^2 \tag{3}$$

(Garstang 1962). The summation in equation (3), extending over the $2J+1$ magnetic quantum numbers, M, can be executed directly using angular momentum techniques. The line strength may then be written

$$S_Q(v'J', v''J'') = \left|\int \Psi^*_{v'J'}(R)Q(R)\Psi_{v''J''}(R)\,dR\right|^2 \times S(J', J'') \quad \text{au}, \tag{4}$$

where the rotational factors are

$$S(J', J'') = \frac{(J''+1)(J''+2)}{2J''+3}$$

S branch: $J' = J''+2$

$$= \frac{2J''(J''+1)(2J''+1)}{3(2J''-1)(2J''+3)}$$

Q branch: $J' = J''$

$$= \frac{J''(J''-1)}{2J''-1}$$

O branch: $J' = J''-2$. (5)

When $Q(R)$ is in atomic units, and the frequency is converted to a transition energy in atomic units, $\varepsilon = \tilde{\nu}/219474.55$, then

$$A(v'J', v''J'') = 8.55474\times 10^4 \varepsilon^5 \times S_Q(v'J', v''J'')/(2J'+1) \quad s^{-1}. \tag{6}$$

The quadrupole moment of H_2 has often been defined to be 2 times larger than would be given by equation (1) (Kołos and Wolniewicz 1965; Dalgarno, Allison, and Browne 1969). Accordingly, our expression for the quadrupole transition probability (6) differs by a factor of 4 from the formulae used by Dalgarno *et al.*, Black and Dalgarno (1976), and Turner, Kirby-Docken, and Dalgarno (1977) for H_2. The rotation-vibration wavefunctions $\Psi_{vJ}(R)$ have been calculated by numerical integration of the radial Schrödinger equation:

$$\frac{d^2}{dR^2}\Psi_{vJ}(R) + 2\mu\left[E_{vJ} - V(R) - J(J+1)/2\mu R^2\right]\Psi_{vJ}(R) = 0, \tag{7}$$

where μ is the reduced mass of C_2 in units of the electron mass, E_{vJ} is the eigenvalue of state (vJ), and $V(R)$ is the potential of the $X\ ^1\Sigma_g^+$ ground state in atomic units. The matrix elements in the line strength (eq. [4]) have been computed using for the determination of Ψ_{vJ} both ab initio and empirical potentials, and these matrix elements agree within a few per cent. An empirical RKR potential (cf. Jarmain 1960) derived from the spectroscopic constants of Marenin and Johnson (1970) has been adopted for the computation of E_{vJ} and Ψ_{vJ}. The transition energies, ε, in equation (6), were determined from these eigenvalues.

TABLE 2

INVERSE RADIATIVE LIFETIMES (quadrupole transitions)

J'	J''	$A_{XX}(0,J';0,J'')$ (s^{-1})	v	$A(vJ)^a$ (s^{-1})
2	0	1.763 (−17)	1	6.46 (−8)
4	2	1.742 (−15)	2	1.30 (−7)
6	4	1.838 (−14)	3	1.96 (−7)
8	6	9.065 (−14)	4	2.62 (−7)
10	8	3.034 (−13)	5	3.27 (−7)
12	10	8.020 (−13)	6	3.90 (−7)
14	12	1.808 (−12)	7	4.51 (−7)
16	14	3.638 (−12)	8	5.08 (−7)
18	16	6.712 (−12)	9	5.61 (−7)
20	18	1.158 (−11)	10	6.11 (−7)

[a]Summed over all transitions to lower levels (cf. eq. [8]); virtually independent of J.

The value of the quadrupole moment at equilibrium internuclear distance is $Q(R_e)=2.26$ au in C_2. The corresponding quadrupole moment of H_2 is $Q_{H_2}(R_e)=0.4574$ au (Kołos and Wolniewicz 1965). The transition frequency of a rotational transition is proportional to the rotation constant, B_e, and enters as the fifth power in the transition probability (eq. [2]). The rotation constant of C_2, $B_e=1.820$ cm^{-1}, is so much smaller than that of H_2, $B_e=60.853$ cm^{-1}, that the rotational lifetimes of C_2 are orders of magnitude longer than the corresponding lifetimes in H_2. The vibrational frequencies of the two molecules are not so different, and the rotation-vibration transition probabilities of C_2 are only slightly smaller than those of H_2. Table 2 contains the pure rotational transition probabilities for $v=0$ and the summed rotation-vibration transition probabilities

$$A(vJ)=\sum_{v''}\sum_{J''}A(vJ,v''J'') \tag{8}$$

for levels with $v\leq 10$, $J\leq 20$. Matrix elements and A values for individual vibrational transitions are available upon request. Typical transition probabilities are $A\approx 2\times10^{-8}$, 3×10^{-9}, and 3×10^{-8} s^{-1} for individual lines in the 1–0 , 2–0, and 2–1 bands, respectively. The lifetimes of levels $(v=0,J)$ are so long that in typical interstellar clouds, rotationally inelastic collisions, and upward electronic transitions will be more efficient in depopulating a level than radiative decay for $J\lesssim 30$.

c) *Intercombination Transitions*

Excited vibrational states of C_2 $X\,^1\Sigma_g^+$ can also decay to lower levels of $a\,^3\Pi_u$ by transitions that occur by the spin-orbit interaction. These levels relax, in turn, by intercombination transitions to the lowest levels of $X\,^1\Sigma_g^+$. Figure 2 is a schematic diagram of energy levels and illustrates the types of transitions among them. Note that the $v=3$ levels of the $X\,^1\Sigma_g^+$ and $a\,^3\Pi_u$ states lie at virtually the same energy. Because of the symmetries of rotational states in a homonuclear molecule with zero nuclear spins, odd-numbered rotational levels do not exist in $X\,^1\Sigma_g^+$, and half of the lambda-doublet levels do not exist in $a\,^3\Pi_u$.

It has been recognized that intercombination transitions will affect the relative strengths of the singlet and triplet systems in the emission spectra of comets (Krishna Swamy and O'Dell 1979). From measurements of the relative strengths of bands of the Mulliken and Swan systems in Comet Bradfield 1979l, A'Hearn and Feldman (1980) have inferred a transition moment-squared of $\Sigma|R_E|^2=(1\text{–}2)\times10^{-5}$ au for $a\,^3\Pi_u-X\,^1\Sigma_g^+$, summed over all independent components. The transition probability for an intercombination line in the Franck-Condon approximation is

$$\begin{aligned}A(v'J',v''J'') &= \frac{64\pi^4}{3h}\tilde{\nu}^3\Big\{\sum|R_E|^2/N_{R_E}\Big\}q_{v'v''}\mathcal{S}_{J'J''}/(2J'+1)\\ &= 2.026\times10^{-6}\tilde{\nu}^3\Big\{\sum|R_E|^2/N_{R_E}\Big\}\\ &\quad\times q_{v'v''}\mathcal{S}_{J'J''}/(2J'+1),\end{aligned} \tag{9}$$

where the square of the transition moment is in atomic units and $q_{v'v''}$ is the Franck-Condon factor (cf. Whiting and Nicholls 1974). The rotational line strengths, $\mathcal{S}_{J'J''}$, are tabulated by Kovacs (1969, Table 3.22) and should be normalized according to the sum rule

$$\sum_{J'}\mathcal{S}_{J'J}=\sum_{J''}\mathcal{S}_{JJ''}=N_{R_E}(2J+1), \tag{10}$$

where the summations extend over all lines having the indicated rotational quantum numbers (Whiting and Nicholls 1974). Single-primed and double-primed quantum numbers always indicate respectively the upper and lower states of a transition, regardless of which electronic state is the upper state. Care must be exercised in applying expressions for rotational line strengths because these depend upon which electronic state is the upper state. The number of independent electronic transition moments, $N_{R_E}=2$ for a $^1\Sigma$–$^3\Pi$ transition (Whiting *et al.* 1973). We assume that the two transition moments are equal in magnitude and independent of internuclear separation, and we adopt $\Sigma|R_E|^2/N_{R_E}=10^{-5}$ au. We have computed Franck-Condon factors

$$q_{v'v''}=\left|\int\Psi_{v'}^*(R)\Psi_{v''}(R)\,dR\right|^2 \tag{11}$$

by numerical integration of the radial wave functions. Accurate RKR potentials based upon the equilibrium constants of Amiot, Chauville, and Maillard (1979) for

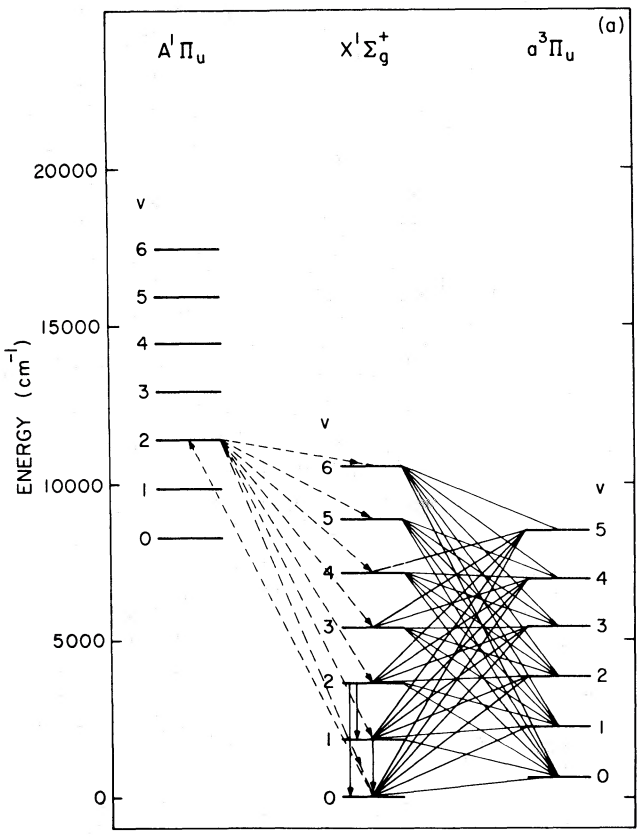

FIG. 2a

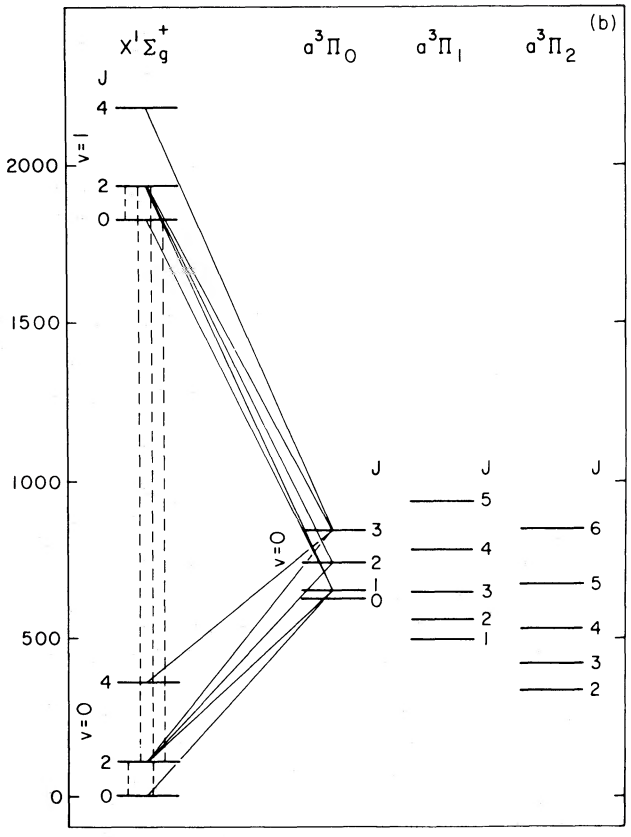

FIG. 2b

FIG. 2.—Low-lying energy levels of C_2. Fig. 2*a* shows the vibrational ladders of the *A*, *X*, and *a* states. The higher-lying *D* and *F* states are not shown. Slanted dashed lines show the allowed fluorescence transitions following absorption in the $A-X$ 2–0 band. Slanted solid lines indicate the intercombination transitions. Vertical solid lines show three of the quadrupole transitions. Fig. 2*b* shows the rotational structure of the three lowest vibrational levels of the molecule. The three $J=0$ levels are positioned to scale; the separations of the other rotational levels have been multiplied by a factor of 10 for clarity. Some quadrupole transitions are indicated by vertical dashed lines. Intercombination transitions are shown by slanted solid lines. Intercombination transitions connecting the $^3\Pi_1$ and $^3\Pi_2$ levels have been omitted for clarity.

a $^3\Pi_u$ ($J=1$) and of Marenin and Johnson (1970) for $X^1\Sigma_g^+$ ($J=0$) have been used in the solution of equation (7) for the wave functions. The Franck-Condon factors are presented in Table 3. For the $X\ ^1\Sigma_g^+$ state, vibration-rotation energy levels were generated from the constants of Marenin and Johnson. Energy levels of the *a* $^3\Pi_u$ state were computed by diagonalization of the Hamiltonian matrix presented as Table II of Amiot *et al.*[2] When we assign zero energy to level $X\ ^1\Sigma_g^+(v=0, J=0)$, the zero level of *a* $^3\Pi_u$ has an energy 612.29 cm^{-1} with an estimated uncertainty of 0.05 cm^{-1} (Veseth 1975). The transition frequencies, $\tilde{\nu}$, in equation (9) were computed from these energy levels based upon accurate spectroscopic data.

[2]There appears to be a typographical error in their expression for the matrix element $\langle {}^3\Pi_0|{}^3\Pi_2\rangle$: the constant *D* should be multiplied by 2 (cf. Cossart, Horani, and Rostas 1977).

With the adopted transition moment, typical values for transition probabilities summed over all possible lower levels are: 3×10^{-2} ($v'=1$), 0.17 ($v'=2$), 0.42 ($v'=3$), and 0.75 s^{-1} ($v'=4$) when $X\ ^1\Sigma_g^+$ is the upper state. When *a* $^3\Pi_u$ is the upper state, typical values are 0.00003–2.0 ($v'=0$), 0.001–0.06 ($v'=1$), 0.003–0.17 ($v'=2$), and 0.006–0.3 s^{-1} ($v'=3$), depending upon the spin component of the upper state. The lowest levels of the F_3 components, $^3\Pi_0$ ($v, J=0$), are all highly metastable because they cannot decay to levels of the *X* state (cf. Fig. 2). In the interstellar medium, there may be some residual population in these levels resulting from the original molecule formation, but this will be small and probably undetectable. Under some conditions, cometary emission lines involving these levels should exhibit anomalous intensities.

Because the vibrational frequencies of the *a* $^3\Pi_u$ and $X\ ^1\Sigma_g^+$ states differ somewhat, there are accidental coincidences between rotational levels of $v=3$ in both

TABLE 3

FRANCK-CONDON FACTORS: C_2 INTERCOMBINATION SYSTEM $a\,^3\Pi_u - X\,^1\Sigma_g^+$

$v(X\,^1\Sigma_g^+)\rightarrow$	0	1	2	3	4	5	6	7	8	9	10
$v(a\,^3\Pi_u)\downarrow$											
0	0.4728	0.3845	0.1222	0.01901	0.00146	0.00005	...	...	...	...	...
1	0.3234	0.03077	0.3451	0.2376	0.05712	0.00581	0.00021	...	...	...	...
2	0.1372	0.2185	0.02025	0.2000	0.3026	0.1071	0.01381	0.00056	...	...	...
3	0.04686	0.1959	0.07655	0.09977	0.07863	0.3153	0.1605	0.02541	0.00110	...	...
4	0.01425	0.1040	0.1679	0.00718	0.1494	0.01461	0.2901	0.2109	0.03996	0.00175	...
5	0.00406	0.04317	0.1368	0.1024	0.00568	0.1497	0.00026	0.2447	0.2543	0.05639	0.00239
6	0.00112	0.01564	0.07574	0.1350	0.04214	0.03711	0.1178	0.01559	0.1936	0.2897	0.07354
7	0.00030	0.00523	0.03415	0.09951	0.1070	0.00762	0.07114	0.07572	0.04209	0.1461	0.3178
8	0.00008	0.00166	0.01362	0.05529	0.1072	0.06843	0.00040	0.09169	0.03880	0.06743	0.1068
9	0.00002	0.00051	0.00503	0.02605	0.07337	0.09845	0.03336	0.01184	0.09507	0.01401	0.08545
10	0.00001	0.00016	0.00177	0.01106	0.04065	0.08372	0.07804	0.01002	0.03094	0.08485	0.00207

states. Intercombination transitions between these closely spaced levels will give rise to an unusual radio frequency spectrum. Estimated frequencies and transition probabilities for a few of these transitions are listed in Table 4. Because of the uncertainty in the singlet-triplet splitting, the tabulated frequencies are of illustrative value only. Such lines might be detectable in a laboratory experiment in which level populations were monitored precisely by optical absorption in allowed electronic transitions, while an intense radio frequency signal was tuned through the microwave region. The level populations would change measurably whenever the system was tuned to one of the transition frequencies. Alternatively, the intercombination lines in the 3–3 or 2–2 bands might be measurable directly by laser magnetic resonance spectroscopy. Such experiments could provide the means of determining the singlet-triplet splitting accurately, and of measuring the intercombination transition moment. Possible astronomical consequences of these lines will be discussed below.

TABLE 4

RADIO FREQUENCY TRANSITIONS

($C_2\,X\,^1\Sigma_g^+ - a\,^3\Pi_u\, v=3 \rightarrow 3$ intercombination band)

$a\,^3\Pi_u$ upper state					
$v'=3$		$v''=3$			
J'	Ω'	J''		ν (GHz)[a]	A (s^{-1})
1	1	0		120.	6.01 (−11)
1	0	2		270.	1.13 (−9)
3	1	2		255.	6.46 (−10)
3	0	4		93.	4.57 (−11)
15	1	14		213.	2.99 (−10)
16	0	16		163.	7.48 (−11)
17	1	16		61.	6.73 (−12)
$X\,^1\Sigma_g^+$ upper state					
$v'=3$		$v''=3$			
J'		J''	Ω''	ν (GHz)[a]	A (s^{-1})
2		1	1	195.	2.43 (−11)
2		2	1	13.	7.52 (−14)
4		4	1	107.	3.08 (−11)
6		5	0	88.	3.20 (−11)
6		6	1	241.	2.46 (−10)
8		7	0	290.	1.18 (−9)
18		18	0	40.	1.09 (−12)
18		19	1	134.	7.35 (−11)

[a] Owing to the uncertainty in the singlet/triplet splitting, these frequencies are of illustrative value only.

d) *Allowed Electronic Transitions*

In interstellar clouds, most of the C_2 exists in $X\,^1\Sigma_g^+$ most of the time. The production of vibrationally and rotationally excited C_2 is initiated by absorption of starlight in the singlet electronic transitions $A\,^1\Pi_u - X\,^1\Sigma_g^+$ (Phillips system), $D\,^1\Sigma_u^+ - X\,^1\Sigma_g^+$ (Mulliken system), and $F\,^1\Pi_u - X\,^1\Sigma_g^+$. These absorptions will be followed by fluorescence to various vibrational levels of $X\,^1\Sigma_g^+$. No other bound states are known which can be reached from the ground state by allowed transitions. It will be shown below that absorption in the Phillips system so dominates the radiative excitation of interstellar C_2 that uncertainties in the properties of the D, F, and possible higher states are not critical. In order to calculate the rates of absorption and the probabilities of fluorescence, the transition moments are needed. The adopted transition moments are summarized in Table 5. There apparently exist no sophisticated theoretical calculations of electronic transition moments for the singlet systems of C_2.

Transition moments have been determined experimentally for the Phillips system by Cooper and Nicholls (1975, 1976) and by Roux, Cerny, and d'Incan (1976). There is a small discrepancy between these two results, and we have adopted a different value from that used by Chaffee *et al.* (1980).

TABLE 5

ELECTRONIC TRANSITION MOMENTS
(Adopted Values)

System	$\Sigma\|R_E\|^2$ (au)	Reference
$A\ ^1\Pi_u - X\ ^1\Sigma_g^+$ ...	0.38	1
$D\ ^1\Sigma_u^+ - X\ ^1\Sigma_g^+$ ...	0.34	2
$F\ ^1\Pi_u - X\ ^1\Sigma_g^+$ ...	0.44	3
$a\ ^3\Pi_u - X\ ^1\Sigma_g^+$	$10^{-5}\ N_{R_E}$	4

REFERENCES.—(1) Cooper and Nicholls 1975, 1976. (2) Curtis *et al.* 1976. (3) Chaffee *et al.* 1980, guess (see text). (4) See text.

Two lifetime measurements (Curtis, Engman, and Erman 1976; Smith 1969) for the $D\ ^1\Sigma_u^+$ upper state of the Mulliken system are in fair agreement. Both of these lifetimes are approximately 3 times smaller than that implied by the shock-tube measurements of Cooper and Nicholls (1975, 1976).

The transition moment adopted for the ultraviolet system, $F\ ^1\Pi_u - X\ ^1\Sigma_g^+$, is a guess appropriate for a typical strong Rydberg transition (cf. Chaffee *et al.* 1980). Upper limits upon the $F-X$ transition moment can be established from astronomical observations. Upper limits exist on the equivalent width of the $F-X$ 0–0 $R(0)$ interstellar line at 1341.63 Å toward ζ Oph (Morton 1975) and toward o Per (Snow 1975). In both directions, C_2 lines in the $A-X$ 2–0 band have been observed (Chaffee and Lutz 1978; Hobbs 1981). Given the upper limits on equivalent width in the $F-X$ system, the measured equivalent widths in the $A-X$ system, and the adopted $A-X$ transition moment, we determine $\Sigma|R_E|^2 < 4.1$ au from both sets of observations. The interstellar $F-X$ 0–0 $R(0)$ lines toward ζ Oph and o Per will appear with equivalent widths of the order of 0.1 to 0.5 mÅ if the transition moment is as small as the assumed value (Table 5).

There continues to be a need for independent experimental studies of the singlet transition moments and for good ab initio theoretical values, especially in the case of the ultraviolet system. Although the variation of $\Sigma|R_E|^2$ with internuclear separation has been determined for the triplet Swan system both experimentally (Danylewych and Nicholls 1974; Tatarczyk, Fink, and Becker 1976) and theoretically (Zeitz, Peyerimhoff, and Buenker 1978; Arnold and Langhoff 1978), there is no indication of significant R variation of singlet transition moments. Thus we assume that the adopted values in Table 5 are all constant.

Oscillator strengths and transition probabilities have been calculated for all important rotational lines of the three singlet systems using the above transition moments. Rotational line strength factors were taken from standard references (Kovacs 1969). RKR Franck-Condon factors were computed for the Phillips system as a test of the computer programs used to generate the radial wavefunctions and matrix elements. These Franck-Condon factors are virtually identical to the results of Dwivedi *et al.* (1978) for $J = 0$. The off-diagonal terms of the Franck-Condon array of the Mulliken system are all so small (Nicholls 1965) that we include only its 0–0 band in the calculation of absorption and fluorescence. We have computed approximate Franck-Condon factors for the $F-X$ system using an empirical potential for the F state which is poorly determined because only two vibrational levels have been observed spectroscopically (Herzberg, Lagerqvist, and Malmberg 1969). For the 0–0 and 1–0 bands, we find $q_{00} = 0.524$ and $q_{10} = 0.314$.

Vibrational levels $v \geq 5$ in $X\ ^1\Sigma_g^+$ lie above some levels of $A\ ^1\Pi_u$ and can therefore decay by strong, allowed electronic transitions more rapidly than by quadrupole or intercombination transitions. Levels this high are negligibly populated by absorption and fluorescence, and the effect of this rapid decay path on the entire cascade will be small.

e) Collisions

Rotationally inelastic scattering of H and H_2 by C_2 can affect the rotational populations. Unfortunately the cross sections for this process are not known. As a first approximation we assume a constant cross section σ_0 for all downward transitions $J+2 \rightarrow J$ (cf. Chaffee *et al.* 1980). Such an approximation provides a reasonably good description of the rates of rotational excitation and de-excitation of H_2 by H and H_2 collisions (cf. Black and Dalgarno 1977). The frequency of de-excitation, $J = 2 \rightarrow 0$, is

$$C(2,0) = 10^4 T^{1/2} n_c \sigma_0 \quad \mathrm{s}^{-1}, \tag{12}$$

where T is the kinetic temperature, n_c is the effective density of collision partners, $n_c = n(\mathrm{H}) + n(\mathrm{H_2})$ in cm^{-3}, and σ_0 is in cm^2. Collisions in which $\Delta v \neq 0$ can be ignored at the temperatures of interest. In the absence of any information about the potential surfaces that describe interactions between C_2 and hydrogen (H or H_2), all collisions in which $\Delta J > 2$ have simply been ignored: this is a valid approximation for describing rotational excitation of H_2 at low temperatures. All other downward rates scale according to the statistical weights

$$C(J+2, J) = C(J, J-2)(2J+1)/(2J+5). \tag{13}$$

The corresponding excitation rates are

$$C(J, J+2) = C(J+2, J) \exp\left[-\Delta E(J+2, J)/kT\right] \times (2J+5)/(2J+1), \tag{14}$$

where ΔE is the energy difference between the two levels. These relations ensure that a thermal population distribution will result in the limit of very high densities (detailed balance).

It is unlikely that the cross section σ_0 will greatly exceed its classical geometrical value, 5×10^{-16} cm^2 for C_2. In an experimental study of reactions involving C_2, Reisler, Mangir, and Wittig (1980) find that C_2 reaches rotational equilibrium at $T=300$ K in 1–3 μs by collisions with He or Ar atoms at pressures of 1–4 torr. This implies a characteristic rotational excitation cross section of the order of $\sigma_0 \approx (1-5)\times10^{-16}$ cm^2. As will be shown below, the observations of interstellar C_2 can be used to place limits upon the product $n_c\sigma_0$. In some interstellar clouds, n_c has been estimated by other means, and the use of C_2 as a diagnostic of density can be calibrated approximately. It would, however, be of great use to have an independent theoretical or experimental determination of the cross section itself.

Several possible excitation processes have been ignored. Quadrupole transitions within the $a\ ^3\Pi_u$ state will be orders of magnitude slower than intercombination transitions and are therefore neglected. Absorptions in other electronic transitions are not considered. In particular, in the Swan system, $d\ ^3\Pi_g - a\ ^3\Pi_u$, the rates of absorption in interstellar clouds are expected to be much smaller than the rates of decay by intercombination transitions. Collisional excitation from $X\ ^1\Sigma_g^+$ to $a\ ^3\Pi_u$ is expected to be inefficient for neutral particle impact compared with collisional excitations within the $X\ ^1\Sigma_g^+$ state. The rates of collisional excitation $X \rightarrow a$ will therefore be small compared with the rates of the absorption, fluorescence, and cascade processes which populate levels of $a\ ^3\Pi_u$. Photodissociation is expected to have a negligible effect on the level populations because its mean interstellar rate is inferred to be 10^{-10} s^{-1} (Black, Hartquist, and Dalgarno 1978), much smaller than the rate of line absorption (see § III*b*, below). In steady state, C_2 is formed at a rate comparable to that of photodissociation; therefore, formation processes are also expected to have insignificant effects on the level populations.

III. ROTATIONAL POPULATIONS IN INTERSTELLAR CLOUDS

In steady state, the populations of the $(v=0, J)$ rotational levels are determined by the balance between the rates of the radiative and collisional processes discussed in § II. The dominant collisional and radiative rates will be shown to be comparable at the densities, $n_c \approx 10^2$ cm^{-3}, and temperatures, $T \approx 20$–100 K, of diffuse interstellar clouds. At much higher densities, the distribution of rotational populations will become thermal and will measure the kinetic temperature of the gas. At low densities or in intense radiation fields, the populations will reflect the probabilities of changing rotational quantum number through absorption, fluorescence, and radiative cascade. In principle, accurate observations of relative rotational populations over a large range of J can be interpreted to reveal the local density, temperature, and strength of radiation field. This analysis of the excitation of C_2 is analogous to that of H_2 (Black and Dalgarno 1976). The radiative cascade in C_2 is somewhat more complicated because it can involve both electric quadrupole and intercombination transitions.

a) Description of Absorption, Fluorescence, and Cascade

In order to describe the radiative excitation of C_2, we define $A_{XX}(v'J', v''J'')$, the probability (s^{-1}) of a quadrupole transition $(v'J') \rightarrow (v''J'')$ within $X\ ^1\Sigma_g^+$; $A_{\alpha\beta}(v'J'\Omega', v''J''\Omega'')$, the probability of an electronic transition from initial electronic state α to final state β; and $A_\alpha(vJ\Omega) = \Sigma_\beta \Sigma_{v''} \Sigma_{J''} \Sigma_{\Omega''} A_{\alpha\beta}(vJ\Omega, v''J''\Omega'')$, the inverse lifetime (i.e., summed transition probability) of a level $(vJ\Omega)$ in electronic state α. The quantum number Ω specifies the spin-multiplet component F_1, F_2, or F_3 ($^3\Pi_2$, $^3\Pi_1$, or $^3\Pi_0$, respectively) in the $a\ ^3\Pi_u$ state, and is not needed to identify singlet levels. The corresponding absorption oscillator strengths for singlet transitions out of initial state $X\ (v=0, J)$ into $\beta(v'J')$ are called $f_{X\beta}(J, v'J')$. The concentration in level $(vJ\Omega)$ of electronic state α is $n_\alpha(vJ\Omega)$ in units of cm^{-3}.

The rate of excitation out of state $X(0, J)$ into state $\beta(v'J')$ is

$$W_{X\beta}(J, v'J') = \frac{\pi e^2}{mc} f_{X\beta}(J, v'J')\phi_\nu \quad \text{s}^{-1}, \qquad (15)$$

where ϕ_ν is the mean intensity of the radiation field (below) at the frequency of the absorption line. This assumes that all absorption lines are optically thin, and that the radiation field is not significantly attenuated by extinction with increasing depth into a cloud. The total absorption rate is

$$W_J = \sum_\beta \sum_{v'} \sum_{J'} W_{X\beta}(J, v'J'). \qquad (16)$$

Concentrations in the excited singlet states, $\beta = A$, D, and F, are

$$n_\beta(v'J') = \sum_{J''} n_X(0J'') W_{X\beta}(J'', v'J')/A_\beta(v'J') \text{ cm}^{-3}. \qquad (17)$$

Populations in levels of $a\ ^3\Pi_u$ are given by the balance between transitions from higher levels of $X\ ^1\Sigma_g^+$ and

transitions to lower levels of $X\,^1\Sigma_g^+$,

$$n_a(vJ\Omega)\sum_{v''\le v}\sum_{J''}A_{aX}(vJ\Omega, v''J'') = \sum_{v'\ge v}\sum_{J'}n_X(v'J')A_{Xa}(v'J', vJ\Omega). \quad (18)$$

The rates of quadrupole and intercombination transitions out of vibrationally excited levels ($v \ge 1, J$) of $X\,^1\Sigma_g^+$ are larger than the rates of collisional processes and allowed electronic absorptions under normal interstellar conditions. Thus the populations for $v \ge 1$ are governed by a purely radiative cascade

$$\begin{aligned} n_X(vJ)A_X(vJ) &= \sum_{v'\ge v}\sum_{J'}n_X(v'J')A_{XX}(v'J', vJ) \\ &+ \sum_{v'\ge v}\sum_{J'}\sum_{\Omega'}n_a(v'J'\Omega')A_{aX}(v'J'\Omega', vJ) \\ &+ \sum_{\alpha=A,D,F}\sum_{v'}\sum_{J'}n_\alpha(v'J')A_{\alpha X}(v'J', vJ). \end{aligned} \quad (19)$$

In the present calculations, the levels $v = 0$–$10, J = 0$–20 of $X\,^1\Sigma_g^+$ have been treated explicitly. When the cascade is purely radiative, its effects upon the populations in ($v = 0, J$) can be described by a cascade matrix $\boldsymbol{C}$ whose elements

$$\begin{aligned} C(v_0J_0; J) &= \sum_{v'}\sum_{J'}n_X(v'J')A_{XX}(v'J', 0J) \\ &+ \sum_{v'}\sum_{J'}\sum_{\Omega'}n_a(v'J'\Omega')A_{aX}(v'J'\Omega', 0J) \end{aligned} \quad (20)$$

give the probability that entry into level (v_0J_0) leads eventually to entry into ($v = 0, J$). This matrix is determined by calculating for each initial level (v_0J_0) a normalized population

$$n_X(v_0J_0) = 1.0/A_X(v_0J_0), \quad (21)$$

and the resulting steady state populations of all lower levels from equation (19). By starting with the highest possible levels, $v_0 = 10$, $J_0 = 20$, and working downward, all the populations and cascade matrix elements can be evaluated directly.

The entire description of radiative excitation of levels ($v = 0, J$) can be simplified further when the cascade is both purely radiative and initiated by optically thin absorptions. The rate of entry into level $X(vJ)$ by fluorescence from levels of the A, D, and F states is

$$P(vJ) = \sum_{\alpha=A,D,F}\sum_{v'}\sum_{J'}n_\alpha(v'J') \times A_{\alpha X}(v'J', vJ) \quad \mathrm{cm^{-3}\,s^{-1}}, \quad (22)$$

where $n_\alpha(v'J')$ is given by equation (17). By summing over all intermediate states, (vJ), we find the rate of population of levels ($v = 0, J_0$) by fluorescence plus cascade to be $\Sigma_v\Sigma_J P(vJ)C(vJ; J_0) + P(0J_0)$. In the optically thin case, the radiative excitation is fully characterized by a matrix $\boldsymbol{Y}$ with elements

$$Y(J_i, J_f) = \left[\sum_v\sum_J P(vJ)C(vJ; J_f) + P(0, J_f)\right] \Big/ \sum_\beta\sum_{v'}\sum_{J'}W_{X\beta}(J_i, v'J') \quad (23)$$

in which the absorption rates $W_{X\beta}$ (eq. [15]) in the denominator must be the same ones used to calculate the fluorescence rates (17) and (22). The matrix $\boldsymbol{Y}$ gives the fraction of absorptions out of level ($v = 0, J_i$) that

TABLE 6

RADIATIVE EXCITATION MATRIX $Y(J_i, J_f)$

	J_f										
J_i	0	2	4	6	8	10	12	14	16	18	20
0.....	5.701 −1	4.064 −1	2.304 −2	4.881 −4	...	...	...	...	...	...	...
2.....	7.720 −2	7.047 −1	2.116 −1	6.442 −3	1.142 −4	...	...	...	...	...	...
4.....	3.915 −3	1.079 −1	7.059 −1	1.779 −1	4.327 −3	7.901 −5	...	...	...	...	...
6.....	1.161 −4	3.881 −3	1.130 −1	7.126 −1	1.664 −1	3.943 −3	7.544 −5	...	...	...	...
8.....	...	7.633 −5	3.000 −3	1.180 −1	7.132 −1	1.617 −1	3.933 −3	7.757 −5	...	...	...
10.....	...	...	5.304 −5	2.904 −3	1.225 −1	7.114 −1	1.591 −1	3.985 −3	8.027 −5	...	...
12.....	...	...	...	5.411 −5	3.224 −3	1.262 −1	7.091 −1	1.573 −1	4.021 −3	8.153 −5	...
14.....	...	...	...	...	6.597 −5	3.662 −3	1.292 −1	7.069 −1	1.560 −1	4.027 −3	8.126 −5
16.....	...	...	...	...	...	8.159 −5	4.102 −3	1.318 −1	7.051 −1	1.549 −1	3.994 −3
18.....	...	...	...	...	...	...	9.826 −5	4.507 −3	1.340 −1	7.071 −1	1.543 −1
20.....	...	...	...	...	...	...	...	1.352 −4	6.262 −3	1.777 −1	8.159 −1

lead to population of $(v=0, J_f)$, and satisfies the condition

$$\sum_{J_f} Y(J_i, J_f) = 1.0. \quad (24)$$

The matrix $\boldsymbol{Y}$ incorporates the frequency dependence of the adopted radiation field, but is otherwise an intrinsic molecular property. This radiative excitation matrix is presented in Table 6. Even though the $a-X$ transition moment is very small (cf. § II*c*), intercombination transitions are more important than quadrupole transitions in controlling the radiative cascade. The values of the matrix elements are quite insensitive to uncertainties in the absolute value of the intercombination transition moment. The excitation matrix would, however, be affected somewhat by a large R dependence of the intercombination transition moment.

b) The Interstellar Radiation Field

Ground-state C_2 absorbs photons in known electronic transitions in the wavelength range 1300–12000 Å, and the rates of these absorptions depend upon the intensity of the interstellar radiation field. The mean radiation field in the ultraviolet has been studied previously by Habing (1968), Witt and Johnson (1973), Jura (1974), and Draine (1978). Recently, Jura (1979) has estimated the mean intensity in the infrared, at $\lambda 2$ μm. The intensities determined for the average galactic radiation field in all of these studies can be represented by the simple formula

$$\phi_\nu = 2.44\times10^{-16}\lambda^{2.7} \text{ photons cm}^{-2}\text{ s}^{-1}\text{ Hz}^{-1} \quad (25)$$

within about 50% at all wavelengths $1000 \lesssim \lambda \lesssim 20000$ Å. We adopt this as the standard field and note that it gives approximately 1.4 times the ultraviolet photon intensity adopted by Black and Dalgarno (1977) in the analysis of the excitation of H_2. Because of the steep wavelength dependence in equation (25), the rates of excitation in the $F-X$ and $D-X$ systems of C_2 will be negligible compared with those in the $A-X$ system. Using equations (15), (16), and (25), we find the total rate of absorption out of levels $(v=0, J)$ to be

$$W_J = 5.7\times10^{-9} \quad \text{s}^{-1}, \quad (26)$$

virtually independent of J. This rate is nearly 7 times larger than that used by Chaffee *et al.* (1980), and the increase is due primarily to the higher background intensity in the near-infrared. For comparison, the collisional excitation frequency is $C(0,2) \approx 4.3\times10^5 n_c\sigma_0 \lesssim 2.1\times10^{-10} n_c$ s^{-1} at $T=100$ K, and $C(0,2) \approx 2.0\times10^4 n_c\sigma_0 \lesssim 1.0\times10^{-11} n_c$ s^{-1} at $T=20$ K; therefore, the collisional and radiative effects are expected to be equally important in the density range $25 \lesssim n_c \lesssim 500$ cm^{-3}. This

TABLE 7

PREDICTED ROTATIONAL POPULATIONS $n_X(0, J)/n_X(0,2)$

J	$n\sigma_0/I$ 10^{-14}	10^{-13}	10^{-12}	THERMAL
		$T=20$		
0.....	0.2687	0.3910	0.4315	0.4371
2.....	1.0	1.0	1.0	1.0
4.....	1.454	0.6251	0.3314	0.2905
6.....	1.800	0.3108	0.0464	0.02389
8.....	2.105	0.1564	0.0048	0.00063
10.....	2.386	0.0839	0.0005	0.00001
12.....	2.640	0.0479	...	...
14.....	2.857	0.0288	...	...
16.....	3.033	0.0180	...	...
18.....	3.155	0.0116	...	...
20.....	3.385	0.0087	...	...
Sum ...	...	2.719	1.815	1.752
		$T=45$		
0.....	0.2392	0.2748	0.2822	0.2831
2.....	1.0	1.0	1.0	1.0
4.....	1.497	0.9635	0.8190	0.8002
6.....	1.825	0.6150	0.3546	0.3234
8.....	2.063	0.3278	0.0958	0.07449
10.....	2.246	0.1647	0.0181	0.01021
12.....	2.386	0.0826	0.0027	0.00085
14.....	2.487	0.0423	0.0003	0.00004
16.....	2.549	0.0224	...	...
18.....	2.568	0.0121	...	...
20.....	2.647	0.0063	...	...
Sum ...	...	3.519	2.573	2.492
		$T=60$		
0.....	0.2312	0.2546	0.2590	0.2595
2.....	1.0	1.0	1.0	1.0
4.....	1.530	1.101	0.9937	0.9800
6.....	1.885	0.8101	0.5736	0.5446
8.....	2.130	0.4836	0.2216	0.1936
10.....	2.306	0.2602	0.0616	0.04597
12.....	2.428	0.1342	0.0132	0.00744
14.....	2.502	0.0686	0.0023	0.00083
16.....	2.534	0.0354	0.0003	0.00006
18.....	2.522	0.0185	...	...
20.....	2.50	0.0086	...	...
Sum ...	...	4.182	3.125	3.032
		$T=100$		
0.....	0.2206	0.2317	0.2336	0.2338
2.....	1.0	1.0	1.0	1.0
4.....	1.593	1.318	1.257	1.250
6.....	2.018	1.214	1.039	1.018
8.....	2.315	0.9091	0.6411	0.6092
10.....	2.513	0.5951	0.3102	0.2798
12.....	2.632	0.3566	0.1215	0.1006
14.....	2.682	0.2015	0.0394	0.02862
16.....	2.674	0.1095	0.0108	0.00649
18.....	2.611	0.0576	0.0025	0.00118
20.....	2.539	0.0265	0.0005	0.00017
Sum ...	52.3	6.040	4.656	4.528

is just the range of densities expected in many diffuse interstellar clouds: it is good fortune that C_2 populations are sensitive to local conditions in just this range.

c) *Equilibrium Rotational Populations*

The steady state concentration in level $(v=0, J)$ of $X\,{}^1\Sigma_g^+$ is given by a set of linear equations

$$\begin{aligned} n_X(0,J)&\left[A_{XX}(0,J;0,J-2)+W_J I+C(J,J+2)\right.\\ &\left.+C(J,J-2)\right]\\ &=n_X(0,J+2)\left[A_{XX}(0,J+2;0,J)+C(J+2,J)\right]\\ &+n_X(0,J-2)C(J-2,J)\\ &+\sum_{J'} W_{J'} I n_X(0,J')Y(J',J). \end{aligned} \tag{27}$$

The parameter I has been introduced as an arbitrary scaling factor in the radiation field. Given the molecular properties calculated above, the values of $n_X(0,J)$ depend parametrically upon the density of collision partners, n_c, the temperature T (through the collision rates), the collisional cross section σ_0, and the strength of the standard radiation field, I. All of the information required to solve equations (27) has been presented in the preceding sections.

In Table 7 we present the population ratios $n_X(0,J)/n_X(0,2)$ for several values of the parameters $n_c\sigma_0$ and T for $I=1.0$. For comparison, the thermal population ratios at the same temperatures are tabulated. Also listed are the total populations relative to that in $v=0$, $J=2$ for those cases in which the summation converges. The reference is taken to be $n_X(0,2)$ rather than $n_X(0,0)$, because the observed column densities tend to have smaller uncertainties for $J=2$ than for $J=0$. It is readily apparent from Table 7 that at low densities (small values of $n_c\sigma_0/I$) the populations mimic those at temperatures rather larger than the kinetic temperature. Even at higher densities, the relative populations of the levels of large J can greatly exceed their thermal values because of radiative excitation.

IV. COMPARISON WITH OBSERVATION

The existing observational data on interstellar C_2 are summarized in Table 8. The relative populations are presented as ratios of column densities, N_J/N_2, for five lines of sight. Where several rotational levels are observed, the populations can be characterized fairly well by a single rotational temperature, $T_{\rm rot}$, as indicated in the table. The preceding analysis suggests that this rotational temperature may not always be close to the kinetic temperature, and that the deviations between T and $T_{\rm rot}$ will become easily discernible at the largest values of J. It is therefore important that future observations include as many rotational levels as possible.

The most extensive observations are those of the diffuse cloud toward ζ Per (Hobbs 1979; Chaffee *et al.* 1980; Cosmovici and Strafella 1981). A model of the ζ Per cloud has been used to infer its physical conditions and predict abundances (Black, Hartquist, and Dalgarno 1978). In the present notation, the molecular core of this cloud model has $n_c=150$ cm^{-3}, $T=45$ K, and $I\approx 0.7$. Theoretical population ratios (cf. Table 7) are in harmony with the observed ratios for $n_c\sigma_0/I=(5\pm2)\times10^{-14}$ at $T=45$ K. The relative populations in the form $-\ln[5N_J/(2J+1)N_2]$ are shown as functions of the excitation energy of level J in Figure 3. If we accept the model parameters, the implied value of the collisional cross section is $\sigma_0\approx 2\times10^{-16}$ cm^2, a reasonable result. Alternatively, if we assumed that $T=T_{\rm rot}$, then a much higher density or a much less intense radiation field, $n_c\sigma_0/I\geq10^{-12}$, would be required for thermalization of the level populations. Such a very large value of $n_c/I\geq$

TABLE 8

INTERSTELLAR C_2: SUMMARY OF OBSERVATIONAL DATA

	N_J/N_2					
J	ζ Per	ζ Per	o Per	ζ Oph	Cyg OB2 No. 12	HD 147889
0	0.2±0.6	0.23±0.05	0.40±0.23	0.23±0.11	0.1±0.1	≲0.3:
2	1.0	1.0	1.0	1.0	1.0	1.0
4	1.2±0.3	1.08±0.23	1.06±0.69	0.91±0.27	0.66±0.30	0.90±0.70
6	<0.9	1.31±0.28	1.40±0.67	1.29±0.49	0.43±0.23	} 0.8
8	...	0.50±0.25	0.48±0.40	0.80±0.21	...	
10	...	0.3±0.3	<0.64	0.46±0.36	...	...
12	...	0.5±0.5	...	<0.3	...	...
$T_{\rm rot}$	78±25	97±10	116±16	130±10	45	60
Reference ...	1	2	3	4	5	5

REFERENCES.—(1) Hobbs 1979. (2) Chaffee *et al.* 1980. (3) Hobbs 1981. (4) Hobbs and Campbell 1982. (5) Souza 1979.

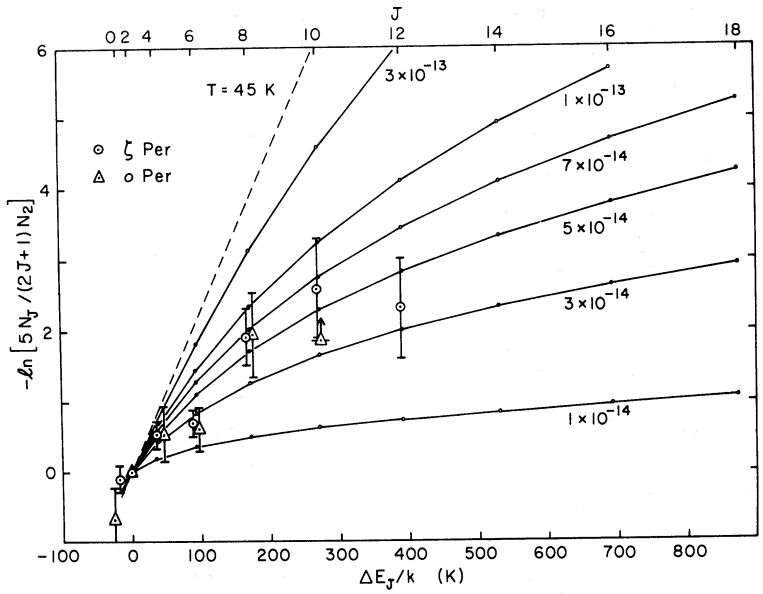

FIG. 3.—Relative rotational populations as functions of excitation energy (or rotational quantum number J) at $T = 45$ K. The theoretical population distributions (*solid curves*) are shown for several values of the parameter $n_c\sigma_0/I$. The dashed line is the thermal distribution at $T = 45$ K. Observational data are displayed for the ζ Per and o Per clouds. Excitation energies are shown relative to that of the $J = 2$ level.

2000, for any reasonable cross section σ_0, would be in severe conflict with the interpretation of the ultraviolet absorption line observations of H_2 and of various atomic species (Black, Hartquist, and Dalgarno 1978).

The predicted level populations can be used to account for the molecules in unobserved levels. At $T = 45$ K, $n_c = 150$ cm^{-3}, $I = 0.7$, and with $\sigma_0 = 2\times10^{-16}$ cm^2, the total column density of C_2 in levels $J = 0$–20 is 5.7 times the column density in $J = 2$. Thus we estimate a C_2 column density toward ζ Per of $N(C_2) = 1.6\times10^{13}$ cm^{-2} from the observations of Chaffee *et al.* (1980) who had found $N(C_2) = 1.2\times10^{13}$ cm^{-2} by assuming a population distribution given by $T = T_{rot} = 97$ K. The prediction of the chemical model of this cloud was $N(C_2) = 1.4\times10^{13}$ cm^{-2} (Black, Hartquist, and Dalgarno 1978). The good agreement between the predicted and observed abundance is partly fortuitous because the rate of a major destruction process, photodissociation, was unknown and had to be guessed. The same photodissociation rate, scaled for a more intense radiation field, provides good agreement between theoretical and observed abundances of C_2 in the ζ Oph cloud (see below). Although the 2 $^1\Pi_u$ state, lying approximately 11.8 eV above the ground state, has been identified theoretically (Kirby and Liu 1979) as a possible photodissociation channel in C_2, it has not been observed spectroscopically, nor has the 2 $^1\Pi_u - X\ ^1\Sigma_g^+$ transition moment been computed. A good estimate of the rate of photodissociation of C_2 is needed. Another uncertainty in the chemical models for the formation of C_2 concerns the previous omission of the reaction

$$C_2 + H_2 \rightarrow C_2H + H \qquad (28)$$

which might be an important destruction mechanism. This reaction occurs with singlet C_2 but not with triplet C_2, and has a rate coefficient of $(1.38\pm.06)\times10^{-12}$ cm^3 s^{-1} at $T = 300$ K (Pasternack and McDonald 1979). It is not known whether this reaction remains rapid at low temperatures; however, on the basis of symmetry considerations, no activation barriers are expected (Reisler *et al.*). If the rate is still 1.4×10^{-12} cm^3 s^{-1} at $T \approx 20$ K, it will remove C_2 almost ten times faster than photodissociation in the core of the ζ Oph cloud. This would not necessarily result in a greatly increased net destruction rate of C_2 because reaction (28) would become a significant source of C_2H. The primary destruction of C_2H by photodissociation

$$C_2H + h\nu \rightarrow C_2 + H \qquad (29)$$

is a major source of C_2, and the formation of C_2 would also occur at an enhanced rate. In other words, reactions (28) and (29) would tend to recycle C_2 with high probability in diffuse clouds. The result of a large rate for reaction (28) at low temperature would be an even larger abundance of C_2H in diffuse clouds than predicted previously. A search for radio lines of C_2H in diffuse clouds where C_2 is seen, and the unambiguous identification of its optical spectrum would be of considerable interest.

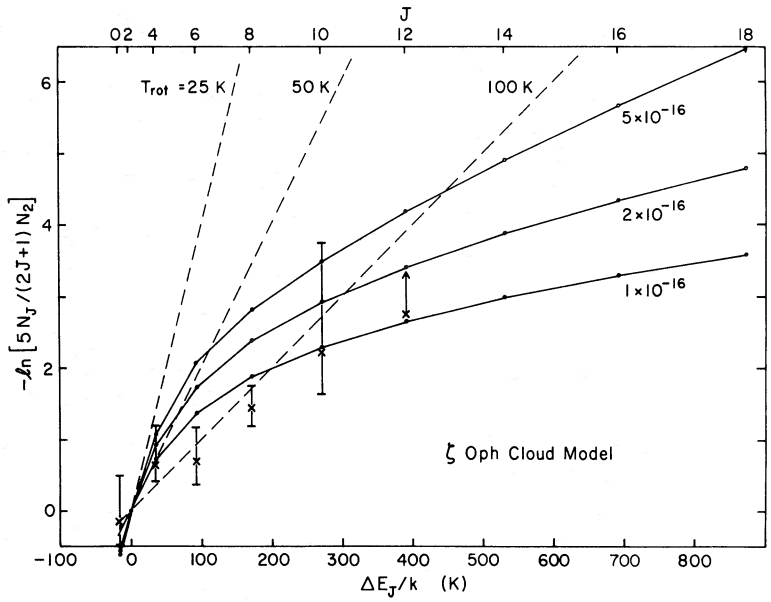

FIG. 4.—Predicted relative rotational populations for a two-component model of the ζ Oph cloud. The three solid curves represent populations for different values of σ_0. The dashed lines indicate thermal distributions. Recent observations of Hobbs and Campbell 1982 are shown for comparison.

The C_2 populations observed toward o Per (Hobbs 1981) are also displayed in Figure 3. It is significant that the relative populations in levels $J=4$, 6, and 8 are virtually identical to those in the ζ Per cloud—indeed, the differences between the two clouds are small compared with the observational uncertainties. This coincidence implies that $n_c\sigma_0/I \approx 5\times10^{-14}$ in both regions, and that the excitation of the lower levels of C_2 is similar in both. Because the two regions belong to the same cloud complex in Perseus, this is not surprising at first glance. These clouds also exhibit similar column densities of H and H_2; however, the higher rotational levels of H_2, $J=4$–6, are much more highly populated toward o Per (Snow 1975, 1976, 1977). The H_2 data suggest that the density is higher and the radiation field stronger in the o Per cloud: $n_c \gtrsim 500$ cm^{-3} and $I \approx 9$ at $T=45$ K (cf. Hartquist, Black, and Dalgarno 1978). Observations of C_2 in even higher rotational levels than already measured toward o Per might reveal a similar effect, and, together with the H_2 data, would help establish the density. We emphasize that an extremely large ratio, $n_c/I \gtrsim 2000$, would be required to explain the observations if the rotational populations were thermalized at $T=T_{rot}=116$ K in the o Per cloud. Again, such a large density or weak radiation field would conflict with the conditions implied by the ultraviolet absorption lines.

Snow (1978) has observed the 0–0 $R(0)$ line of the Mulliken system toward ζ Oph and has determined an upper limit to the strength of the $R(2)$ line. These data imply an upper limit on the rotational temperature, $T_{rot} \lesssim 26$ K, at the significance level of two standard deviations in the statistical uncertainties. The observation of a line from $J=2$ in the Phillips system (Chaffee and Lutz 1978) cannot be used to determine the population ratio with any precision because of lingering uncertainties in the oscillator strengths. In a model of the ζ Oph cloud (Black and Dalgarno 1977), a fraction 0.12 of the C_2 exists in a warm zone with $n_c \approx 400$ cm^{-3} and $T=110$ K, while the remaining C_2 lies in a cold zone with $n_c \approx 1335$ cm^{-3} and $T=22$ K. In the present notation, $I=1.8$. The theory developed here together with the earlier cloud model can be used to predict a rotational temperature for $J=0$ and $J=2$, $T_{02}=26$–30 K, for collisional cross sections in the range $\sigma_0=(1$–$5)\times10^{-16}$ cm^2. Thus the model is marginally consistent with Snow's (1978) observations. In Figure 4 we present the predicted rotational population distribution for the ζ Oph cloud model. The populations in levels $J=0$–6 are characterized by $T_{rot} \approx 25$–50 K, while the populations of the higher levels, $J \geq 6$, are given by $T_{rot} \approx 50$–100 K. After this paper was submitted for publication, we received a preprint (Hobbs and Campbell 1982) reporting new observations of C_2 in rotational levels $J=0$–10 (cf. Table 8). These new observational data are displayed in Figure 4, and they agree well with the predicted populations for a value of the cross section, σ_0, slightly less than 1×10^{-16} cm^2. In particular, the prediction that the rotational excitation temperature $T_{rot} \gtrsim 50$ K for $J \geq 6$ is substantiated by the new observations.

C_2 has also been observed toward Cyg OB2 No. 12 and HD 147889 by Souza (1979) and toward Cyg OB2

No. 12, ζ Per, o And, ζ Oph, and ν Cyg by Cosmovici and Strafella (1981), but meaningful inferences of densities and temperatures cannot be made from these data.

As impressive as the existing observations are, they do not yet permit the extraction of T, n_c, and I independently and directly as do the ultraviolet observations of H_2. With an independent determination of the kinetic temperature, the ratio n_c/I can easily be found from C_2 observations. There remains an uncertainty in the cross section, σ_0, but its value has been calibrated approximately in terms of a model analysis of the ζ Per cloud. If the destruction of C_2 were fully understood, its total column density relative to A_v (which is proportional to the total hydrogen column density) might also be an indicator of n_c/I, so that n_c and I could both be determined. A sample of interstellar clouds could be classified according to the parameter n_c/I on the basis of a survey of C_2 absorption lines, provided that T could be estimated otherwise. It is reasonable to expect a low and relatively uniform temperature, $T \approx 15$–25 K, in fairly thick diffuse clouds having visual extinctions $A_v \gtrsim 1$ mag.

The far-infrared and radio frequency spectrum of C_2 predicted in § II*c* is of possible astronomical interest. A measurement of the intercombination transition moment is needed for the analysis of the excitation of C_2 in comets as well as in interstellar clouds. Precise determinations of the transition frequencies would permit searches for these lines in astronomical sources. The abundance of vibrationally excited C_2 will be very small in normal interstellar clouds, although very close to an infrared source the radiative excitation rates could be quite large. Because the populations of vibrationally excited levels will be nonthermal in general, maser amplification of some transitions may occur under special circumstances.

Radio line emission has been observed from vibrationally excited molecules in circumstellar envelopes. The identification of circumstellar SiO is secure, and its rotational transitions appear to be excited radiatively, in part. Scoville and Solomon (1978) have identified a line in the carbon-rich object IRC +10216 as the $v=1$, $J=1 \rightarrow 0$ rotational line of CO and have attributed it to a radiatively pumped maser region near the stellar surface. This identification has been questioned by Cummins, Morris, and Thaddeus (1980). If we assume (as did Scoville and Solomon) that the underlying photosphere radiates like a blackbody at $T_* = 2000$ K, then the rates of radiative excitation in the Phillips system of C_2 are $W_J \approx 200 r^{-2}$ s^{-1} where r is the distance from the star in units of the photospheric radius. Out to $r \lesssim 20$, these radiative excitation rates exceed the spontaneous decay rates, and vibrational states $v=2$ and $v=3$ can be significantly populated. The excited molecules may be distributed over a large number of rotational levels so that far-infrared and radio lines in the $X\ ^1\Sigma_g^+ \leftrightarrow a\ ^3\Pi_u$ 3–3 and 2–2 bands will probably be undetectably weak in the absence of maser amplification.

C_2 is also observed in the visible spectra of comets. Excited vibrational states can be populated by solar fluorescence, and the intensities of intercombination lines can, in principle, be predicted directly from observed intensities of fluorescence lines in the Swan system. In steady state, the emission rate of Swan system lines terminating in a level of $a\ ^3\Pi_u$ ($v=2$ or $v=3$) is equal to the decay rate from that level. These rates are typically of the order of 10^{-1} s^{-1}. The intercombination transitions $a\ ^3\Pi_u \rightarrow X\ ^1\Sigma_g^+$ arising in these levels have transition probabilities ranging from 10^{-12} to 10^{-6} s^{-1}. Therefore, the intercombination line emission rate will be a small fraction, $<10^{-5}$, of the emission rate of a single line in one of the Swan bands.

This work has been supported by the U.S. National Science Foundation under grant AST-79-06373, and by the Netherlands Organization for the Advancement of Pure Research (ZWO). We are grateful to A. Dalgarno, T. de Jong, H. J. Habing, and M. C. van Hemert for comments on the manuscript. We thank K. Kirby for providing a computer program to calculate rotation-vibration wavefunctions. We thank L. M. Hobbs and P. Erman for providing copies of their work prior to publication.

Note Added in Manuscript.—While this work was in process of publication, new measurements of oscillator strengths for the Phillips system (Erman *et al.* 1982) came to our attention. These oscillator strengths are somewhat smaller than the values adopted here, and the transition moment is found to vary measurably with internuclear distance. Ab initio calculations (E. van Dishoeck, in preparation) also indicate that the adopted oscillator strength is too large, although not by as large a factor as the new experimental results suggest. However, the R dependence of the theoretical transition moment is opposite to that found by Erman *et al.* (1982); that is, the calculated transition moment decreases with internuclear distance. The R dependence of the transition moment has a negligible effect upon the fluorescence and cascade probabilities, and the new oscillator strengths can be incorporated into the above analysis by a simple scaling procedure. The adopted absorption rate, W_J (eq. [26]), is 1.8 times larger than would be the case with the new experimental oscillator strengths for the Phillips system (Erman *et al.* 1982), and 1.3 times larger for the theoretical oscillator strengths. The parameter $n_c\sigma_0/I$ should therefore be divided by 1.8 or 1.3, respectively, if the new oscillator strengths are used.

REFERENCES

A'Hearn, M. F. and Feldman, P. D. 1980, *Ap. J.* (*Letters*), **242**, L187.
Amiot, C., Chauville, J., and Maillard, J.-P. 1979, *J. Molec. Spectrosc.*, **75**, 19.
Arnold, J. O., and Langhoff, S. R. 1978, *J. Quant. Spectrosc. Rad. Transf.* **19**, 461.
Black, J. H. and Dalgarno, A. 1973, *Ap. J.* (*Letters*), **184**, L101.
_____. 1976, *Ap. J.*, **203**, 132.
_____. 1977, *Ap. J. Suppl.*, **34**, 405.
Black, J. H., Hartquist, T. W., and Dalgarno, A. 1978, *Ap. J.*, **224**, 448.
Chaffee, F. H., Jr., and Lutz, B. L. 1978, *Ap. J.* (*Letters*), **221**, L91.
Chaffee, F. H., Jr., Lutz, B. L., Black, J. H., Vanden Bout, P. A., and Snell, R. L. 1980, *Ap. J.*, **236**, 474.
Clementi, E., and Roetti, C. 1974, *Atomic Data Nucl. Data Tables*, **14**, 177.
Cooper, D. M., and Nicholls, R. W. 1975, *J. Quant. Spectrosc. Rad. Transf.*, **15**, 139.
_____. 1976, *Spectrosc. Letters*, **9**, 139.
Cosmovici, C. B., and Strafella, F. 1981, *Astr. Ap.*, **98**, 408.
Cossart, D., Horani, M., and Rostas, J. 1977, *J. Molec. Spectrosc.*, **67**, 283.
Cummins, S. E., Morris, M., and Thaddeus, P. 1980, *Ap. J.*, **235**, 886.
Curtis, L., Engman, B., and Erman, P. 1976, *Phys. Scripta*, **13**, 270.
Dalgarno, A., Allison, A. C., and Browne, J. C. 1969, *J. Atmos. Sci.*, **26**, 946.
Danylewych, L. L. and Nicholls, R. W. 1974, *Proc. Roy. Soc. London*, *A*, **339**, 197.
Draine, B. T. 1978, *Ap. J. Suppl.*, **36**, 595.
Dwivedi, P. H., Branch, D., Huffaker, J. N., and Bell, R. A. 1978, *Ap. J. Suppl.*, **36**, 573.
Erman, P., Lambert, D. L., Larsson, M., and Mannfors, B. 1982, *Ap. J.*, **253**, 983.
Garstang, R. H. 1962, in *Atomic and Molecular Processes*, ed. D. R. Bates (New York: Academic Press), p. 1.
Glassgold, A. E., and Langer, W. D. 1974, *Ap. J.*, **193**, 73.
Habing, H. J. 1968, *Bull. Astr. Inst. Netherlands*, **19**, 421.
Hartquist, T. W., Black, J. H., and Dalgarno, A. 1978, *M.N.R.A.S.*, **185**, 643.
Herzberg, G., Lagerqvist, A., and Malmberg, C. 1969, *Canadian J. Phys.*, **47**, 2735.
Hobbs, L. M. 1979, *Ap. J.* (*Letters*), **232**, L175.
_____. 1981, *Ap. J.*, **243**, 485.
Hobbs, L. M., and Campbell, B. 1982, *Ap. J.*, **254**, 108.
Jarmain, W. R. 1960, *Canadian J. Phys.*, **38**, 217.
Jura, M. 1974, *Ap. J.*, **191**, 375.
Jura, M. 1975*a*, *Ap. J.*, **197**, 575; erratum **202**, 561.
_____. 1975*b*, *Ap. J.*, **197**, 581.
_____. 1979, *Ap. Letters*, **20**, 89.
Kirby, K., and Liu, B. 1979, *J. Chem. Phys.*, **70**, 893.
Kołos, W., and Wolniewicz, L. 1965, *J. Chem. Phys.*, **43**, 2429.
Kovacs, I. 1969, *Rotational Structure in the Spectra of Diatomic Molecules* (New York: American Elsevier).
Krishna Swamy, K. S., and O'Dell, C. R. 1979, *Ap. J.*, **231**, 624.
Marenin, I. R., and Johnson, H. R. 1970, *J. Quant. Spectrosc. Rad. Transf.*, **10**, 305.
Morton, D. C. 1975, *Ap. J.*, **197**, 85.
Nicholls, R. W. 1965, *J. Res. NBS*, **69A**, 397.
Pasternack, L., and McDonald, J. R. 1979, *Chem. Phys.*, **43**, 173.
Reisler, H., Mangir, M. S., and Wittig, C. 1980, *J. Chem. Phys.*, **73**, 2280.
Roux, F., Cerny, D., and d'Incan, J. 1976, *Ap. J.*, **204**, 940.
Sanner, F., Snell, R., and Vanden Bout, P. 1978, *Ap. J.*, **226**, 460.
Scoville, N. Z., and Solomon, P. M. 1978, *Ap. J.* (*Letters*), **220**, L103.
Smith, W. H. 1969, *Ap. J.*, **156**, 791.
Snow, T. P., Jr., 1975, *Ap. J.* (*Letters*), **201**, L21.
_____. 1976, *Ap. J.*, **204**, 759.
_____. 1977, *Ap. J.*, **216**, 724.
_____. 1978, *Ap. J.* (*Letters*), **220**, L93.
Souza, S. P. 1979, Ph.D. thesis, State University of New York, Stony Brook.
Souza, S. P., and Lutz, B. L. 1977, *Ap. J.* (*Letters*), **216**, L49; erratum **218**, L31.
Spitzer, L., Jr., and Jenkins, E. B. 1975, *Ann. Rev. Astr. Ap.*, **13**, 133.
Tatarczyk, T., Fink, E. H., and Becker, K. H. 1976, *Chem. Phys. Letters*, **40**, 126.
Turner, J., Kirby-Docken, K., and Dalgarno, A. 1977, *Ap. J. Suppl.*, **35**, 281.
Veseth, L. 1975, *Canadian J. Phys.*, **53**, 299.
Watson, W. D. 1974*a*, *Ap. J.*, **188**, 35.
_____. 1974*b*, *Ap. J.*, **189**, 221; erratum: **191**, 797.
Whiting, E. E., and Nicholls, R. W. 1974, *Ap. J. Suppl.*, **27**, 1.
Whiting, E. E., Paterson, J. A., Kovacs, I., and Nicholls, R. W. 1973, *J. Molec. Spectrosc.*, **47**, 84.
Witt, A. N., and Johnson, M. W. 1973, *Ap. J.*, **181**, 363.
Zeitz, M., Peyerimhoff, S. D., and Buenker, R. J. 1978, *Chem. Phys. Letters*, **58**, 487.

JOHN H. BLACK: Harvard-Smithsonian Center for Astrophysics, 60 Garden Street, Cambridge, MA 02138

EWINE F. VAN DISHOECK: Sterrewacht-Huygens Laboratorium, Wassenaarseweg 78, 2300 RA Leiden, The Netherlands